The American Journal of Pathology, Vol. 180, No. 5, May 2012

DOI: 10.1016/j.ajpath.2012.01.014

Biomarkers, Genomics, Proteomics, and Gene Regulation

MicroRNA 15a, Inversely Correlated to PKCα, Is a Potential Marker to Differentiate between Benign and Malignant Renal Tumors in Biopsy and Urine Samples

Melanie von Brandenstein,*
Jency J. Pandarakalam,* Lukas Kroon,*
Heike Loeser,* Jan Herden,† Gabriele Braun,†
Katherina Wendland,* Hans P. Dienes,*
Udo Engelmann,† and Jochen W.U. Fries*

From the Institutes of Pathology and Urology,† University Hospital, Cologne, Germany*

NF-κB signal transduction is a potential therapeutic target in many malignant tumors. We have recently shown, in malignant renal proximal tumor cells, that a transcription complex, consisting of NF-κB p65 and mitogen-activated protein kinase p38α, joined by protein kinase C (PKC) α, transmigrates into the nucleus. There, PKCα suppresses the nuclear release of primary microRNA (pri-miRNA) 15a. Induced by endothelin (ET)-1, a decrease in PKCα levels leads to increased miRNA 15a (miR-15A) expression. An identical system can be identified in renal carcinomas, in which, after nuclear transmigration, PKCα binds directly to pri-miRNA 15a in the nucleus. However, the pattern of PKC isoforms differs between malignant renal cell carcinoma (RCC) and benign oncocytoma. PKCα, a component of the transcription complex in tumors, is up-regulated in benign oncocytoma but down-regulated in RCC. Conversely, miRNA 15a is up-regulated in RCC and down-regulated in oncocytoma. A similar behavior is observed in chromophobe carcinoma, whereas differences are less pronounced in papillary RCC (type I): NF-κB target gene expression (ie, ET-1, ET-A and ET-B receptors, vascular cell adhesion molecule-1, IL-6, and fractalkine) is particularly high in malignant RCCs. Up-regulated miRNA 15a can be measured in urine from patients with RCC but is nearly undetectable in oncocytoma, other tumors, and urinary tract inflammation. Thus, the up-regulation of miRNA 15a may be an important marker to help identify malignant clear-cell RCCs in both biopsy and urine samples. ***(Am J Pathol 2012, 180:1787–1797; DOI: 10.1016/j.ajpath.2012.01.014)***

MicroRNAs (miRNAs) are short, noncoding RNAs that can play important roles in cell function and development by targeting mRNA sequences of protein-coding transcripts, resulting in either mRNA cleavage or repression of productive translation.[1–4] Several hundred miRNAs have been discovered in mammals[5,6] and in the human genome through computational and cloning approaches.[7] Calin et al[8] reported that human miRNA genes are frequently located in fragile sites and genomic regions involved in cancer. In this context, Cohen et al[9] found that the α isoform of protein kinase C (PKC) is able to down-regulate miRNA 15a (miR-15a) in head and neck squamous cell carcinoma, identifying this miRNA as a potential inhibitor of DNA synthesis and PKCα as a key regulator of tumor cell growth in squamous cell carcinoma. In addition, miRNA 15a has been described as a tumor suppressor, promoting apoptosis and inhibiting cell proliferation[10] (eg, in multiple myeloma[11] and prostate cancer).[12] Thus, it seems that modulation of miRNA activity in human cancer could be a new approach for cancer gene therapy.[13] A role for miRNAs in renal cell carcinomas (RCCs) has not been proposed.

Endothelin (ET)-1, first described as a vasoconstrictor peptide,[14] has been a potent mitogen for normal human renal tubular epithelial cells[15] and renal interstitial fibroblasts.[16] ET-1 binds via two independent receptors, A and B; the former mediates cell proliferation and vasoconstriction, and the latter presumably mediates vasodilatation, natriuresis, and ET clearance.[17–19] In normal human kidneys, ET-1 and ET receptors have been demonstrated in human proximal tubule cells.[20] ET-1–mediated signal transduction has been linked to the induction of an inflammatory signal transduction cascade via the pleiotropic NF-κB family of dimeric transcription factors. Recently, we have shown that mitogen-activated protein kinase (MAPK) p38 associates with NF-κB p65 after ET-1 stimulation to form a transcription

Supported by a postdoctoral fellowship from Koeln-Fortune (M.v.B.) and a grant from Marga and Walter Boll Stiftung (J.W.U.F.).

Accepted for publication January 10, 2012.

Address reprint requests to Jochen W.U. Fries, M.D., Division of Molecular Nephropathology, University of Cologne, Institute of Pathology, Kerpenerstrasse 62, 50931 Koeln, Germany. E-mail: jochen.fries@uni-koeln.de.

complex (TC) in the cytoplasm.[21] Nuclear translocation induces expression of a variety of genes containing an NF-κB binding site in their promoter.

MAPK p38 participates in a signaling cascade controlling cellular responses to cytokines and stress. Four isoforms of p38 have been identified: p38α (MAPK14), p38β (MAPK11), p38γ (MAPK12 or extracellular signal–regulated kinase 6), and p38δ (MAPK13 or stress-activated protein kinase 4).[22] Although an interaction between p38 and NF-κB has been described earlier for IL-6 regulation,[21,23] we recently showed that p38α forms a TC with NF-κB p65 already in the cytoplasm, migrating as a complex into the nucleus, where it regulates the expression of genes with NF-κB target sites, such as vascular cell adhesion molecule-1, IL-6, and fractalkine.[20]

PKC has been identified as an important signaling pathway in a wide variety of cell types.[24–26] This serine-threonine kinase has been associated with signal transduction pathways, resulting in cell differentiation and division, contraction, and secretion.[24,25] At present, 13 members of the PKC family of protein kinases have been identified on the basis of structural similarities. The individual members of this family have been classified into three groups: the classical PKCs (α, βI, βII, and γ), the novel PKCs, and the atypical PKCs (aPKCs).[26] The C1 region of the classical PKCs contains two cysteine-rich, zinc-finger motifs separated by 8 to 15 residues. These two zinc finger–like motifs are thought to synergistically provide for the ability to bind to and to be activated by diacylglycerol.[24] Our research group has determined that, at 24 hours after ET-1 induction, an ET-1 receptor–independent signaling occurs via diacylglycerol, resulting in a second peak of gene expression[20] in different tumor and normal cell lines. In humans, the same PKC isoforms were detected in normal kidneys as in RCC cell lines (Engers et al[27]: PKCs α, ε, ξ, μ, and í) and were missing PKCδ. In the study by Engers et al, expression of PKCα and PKCε was associated with highly invasive potential. In human RCCs, Brenner et al[28] confirmed the importance of PKCη, whereas PKCα was decreased in tumor versus normal tissue.

RCC is the most common neoplasm affecting the adult human kidney and the third most common urologic malignancy (after bladder and prostate carcinoma), representing 2% to 3% of all malignancies worldwide. RCCs are a heterogeneous group of malignancies. The major subtypes are clear-cell, papillary, and chromophobe (CP) RCCs.[29] Of these RCCs, the clear-cell subtype represents approximately 70% to 80% of patients' renal carcinoma, whereas papillary RCC is reported only in 10% to 15% of patients. CP RCC, constituting 5% to 10% of carcinoma, is the least common and has morphological features overlapping with oncocytoma, a benign neoplasm.[30] The distinction between these two tumors is clinically important, because CP RCC, although considered to have a better prognosis than clear-cell RCC,[30] is malignant and can be potentially aggressive. Differences in the behavior have been related, in part, to ET-1, which reportedly promotes cell survival in RCC through an ET-A receptor[31] in different renal tumor cell lines. Major differences in endothelial axis expression have been reported between clear-cell and papillary subtypes,[32] where papillary RCCs have significantly less ET-A receptor, preproendothelin, and endothelin-converting enzyme. As another important signaling pathway in RCC, p38 has played a role in cell proliferation and apoptosis.[1,33]

We recently proposed that a signaling loop exists linking miRNA 15a, PKCα, MAPK p38, NF-κB p65, and ET-1 together, resulting in regulation of NF-κB–mediated gene expression.[34] We suggested that, in resting cells, a TC of NF-κB and MAPK p38 is joined by PKCα, where, after nuclear transmigration, PKCα suppresses the release of pri-miRNA 15a by direct molecular interaction. If the cell is stimulated by ET-1, the amount of PKCα decreases, allowing the generation of mature miRNA 15a. This signaling could be found in different tumor cell lines, among them Caki-1, a cell line established from RCC.

Thus, we investigated whether the same signaling loop is present in different renal cell tumor types (malignant clear cell, CP, and papillary versus benign oncocytoma), whether classical target genes of NF-κB are activated and whether the ET-1 system and its receptors are involved, because RCCs are known for ET-1 expression. We found that miRNA 15a levels from paraffin-embedded tissue samples and, most important, from urine samples are inversely related in malignant versus benign renal tumors. This finding represents a potential new marker for clear-cell RCC versus oncocytoma differentiation in biopsy samples and preoperatively in urine of patients with renal cancer.

Materials and Methods

Renal Tumors and Urinary Samples

Formalin-fixed and paraffinized human renal tissue samples from the archives of the Department of Pathology, University Hospital of Koeln, Koeln, Germany, were used. Histological evaluation was based on analyses by two staff pathologists (H.P.D. and J.W.U.F.) independently using H&E-stained paraffin sections. A total of 23 renal tumors were used [renal clear-cell carcinoma (n = 7), CP renal carcinoma (n = 5), renal papillary cell carcinoma (n = 6), and renal oncocytoma (n = 5)]. Normal renal tissue was taken from explanted, but not transplanted, donor kidneys (no allocation in time) (n = 5). The Fuhrmann grade of renal carcinoma was one to two times higher, or tumors with sarcomatoid differentiation were excluded. Areas of necrosis or fibrosis were macrodissected and discarded.

Fresh tumor tissue was procured in the context of performing a frozen section for tumor diagnosis from either clear-cell renal carcinoma or oncocytoma, snap frozen in liquid nitrogen, and stored at −80°C until use.

Urine Collection

Urine samples of approximately 50 to 100 mL were selected from patients according to diagnosis shown in Table 1. In patients with tumor, urine was collected at two different time points (before operation and at hospital release). All urine was frozen at −20°C until further use.

Table 1. Patient Data for Cases with Analyses of Formalin-Fixed Paraffininzed Human Tissue

Patient no.	Diagnosis	Sex	Age (years)	Tumor size (cm)
1	Onco	F	79	1.5
2	Onco	M	49	4
3	Onco	M	71	2
4	Onco	M	68	10.0
5	Onco	M	74	5
6	CP	M	63	5.5
7	CP	M	81	2.3
8	CP	M	64	3.3
9	CP	F	55	4
10	CP	F	70	2.8
11	PAPI	M	74	1.5
12	PAPI	M	45	3.0
13	PAPI	M	56	1.5
14	PAPI	M	78	6
15	PAPI	F	62	3.1
16	PAPI	M	76	2.2
17	RCC	M	73	2.2
18	RCC	F	53	5.5
19	RCC	F	59	6.0
20	RCC	F	73	4.0
21	RCC	M	70	2.0
22	RCC	F	63	3.7
23	RCC	M	66	1.5
24	Normal		Control paraffin-embedded tissues	
25	Normal		Control paraffin-embedded tissues	
26	Normal		Control paraffin-embedded tissues	
27	Normal		Control paraffin-embedded tissues	
28	Normal		Control paraffin-embedded tissues	

F, female; M, male; CP, chromophobe RCC; Onco, oncocytoma; PAPI, papillary RCC.

Because human materials (renal tissue and urine) were used, procedures were followed as outlined in accordance with ethical standards formulated in the Declaration of Helsinki 1975, with preapproval by the Ethics Committee at the University Hospital, Koeln (reference no. 09-232).

Immunohistological Characteristics

Paraffin-embedded tissue sections (4 μm thick) were deparaffinized by incubation for 2 $\times$ 5 minutes in xylene, followed by 2 $\times$ 3 minutes in 100% ethanol, and 1 minute in 95% ethanol; and then rinsed with distilled water. The slides were incubated with a specific serum blocker (anti-rabbit) for 30 minutes, to avoid unspecific binding. After that incubation period, the slides were re-incubated for 1 hour at room temperature with specific primary antibodies (PKCα/PKCβII; Santa Cruz, Heidelberg, Germany). After washes with PBS–Tween 20, sections were incubated with a secondary anti-rabbit antibody (Santa Cruz). After rinsing with PBS–Tween 20, slides were re-incubated for 2 minutes in 95% ethanol, followed by 2 $\times$ 3 minutes in 100% methanol, counterstained with H&E, and coverslipped.

Nonradioactive EMSA

Nuclear extracts (NEs) were isolated from fresh tissue samples according to the manufacturer's protocol (Nuclear Extraction Kit; Active Motif, Carlsbad, CA). Protein content was assayed with the Bradford protein assay (Bio-Rad, Munich, Germany) with bovine serum albumin as standard. Double-stranded pri-miRNA 15a oligonucleotides (5′-TGTGGATTTTGAAAAGG-3′) were commercially synthesized (Invitrogen, Darmstadt, Germany), and the forward strand was labeled with Alexa 647. Pri-miRNA 15a binding reactions were conducted in 200 mmol/L Tris-HCL, pH 7.6, 50 mmol/L $MgCl_2$, 0.1 mmol/L EDTA, and 10 mmol/L dithiothreitol. To prepare the DNA for annealing, the oligonucleotides (1 pmol each) were incubated at 70°C for exactly 10 minutes and for a further 30 minutes at room temperature. For the protein/RNA binding reaction, 5 μg of protein was added to the samples and incubated on ice for 30 minutes. The reaction was analyzed by electrophoresis in a nondenaturation 6% polyacrylamide gel in 1$\times$ TRIS-Borat-EDTA (TBE) buffer.

For supershift electrophoretic mobility shift assays (EMSAs), a PKCα antibody (Santa Cruz) was used. As negative control, 100$\times$ more concentrated, nonlabeled pri-miRNA 15a was incubated with 5 μg of protein and added to the Alexa-labeled sample. As binding and negative control, a mutated pri-miRNA 15a oligo (Alexa 647, 5′-GTGTTCGGGGTCCCCTT-3′; Invitrogen) was used as well. All EMSAs were performed in triplicate and visualized with a fluorescence reader (Licor, Bad Homburg, Germany).

Immunoprecipitation

For immunoprecipitation, a MAPK p38 agarose conjugated antibody (Santa Cruz) was used as previously described[21] and incubated with 250 ng of nuclear extracts

Table 2. Primers Used in this Study

Name	Forward primer	Reverse primer	Cycles	Temperature (°C)
β-Actin	5′-TTGGCAATGAGCGGTTCCGCTG-3′	5′-TACACGTGTTTGCGGATGTCCAC-3′	45	53
PKCα	5′-ATGGCTGACGTTTTCCCGG-3′	5′-AGGTGGGCTGCTTGAAGA-3′	45	55
ET-1	5′-CCAAGGAGCTCCAGAAACAG-3′	5′-GATGTCCAGGTGGCAGAAGT-3′	45	55
IL-6	5′-GCTATGAACTCCTTCTCCACAAGCG-3′	5′-TGAAGAGGTGAGTGGCTGTC-3′	45	53
ET-A receptor	5′-AGCTCAGCTTCCTGGTTACC-3′	5′-TCCTGAGCAGAGTTGCATTC-3′	45	55
ET-B receptor	5′-GCCATTTGGAGCTGAGATGT-3′	5′-CTGCTGTCCATTTTGGAACC-3′	45	55
Fractalkine	5′-CAGAGGAGAATGCTCCGTCTG-3′	5′-GGTCCCTTCTGAGGAAGACAG-3′	45	53
VCAM	5′-GGCCCAGTTGAAGAATGCGG-GAGTATATG-3′	5′-GATTTCTGTGCTTCTACAAG-ACTATATGACCC-3′	45	55

VCAM, vascular cell adhesion molecular.

from either normal tissue (positive control) oncocytoma or RCC. The samples were washed twice with 1× PBS, and SDS-PAGE was performed. As negative control, only agarose beads were used.

Immunoprecipitation and PCR

The immunoprecipitation was performed with 250 ng of NE of each tumor type and incubated with an agarose-conjugated PKCα antibody. As negative control only, agarose beads were used. After the incubation step, the samples were washed twice with 1× PBS, the RNA was isolated and reverse transcribed, and a PCR with pri-miRNA 15a–specific primers was performed. The product was loaded on a 3% agarose gel, and the band of the expected size was isolated and sequenced by the Sanger method.

miRNA Isolation

For miRNA isolation of the formalin-fixed, paraffin-embedded (FFPE) samples, the RNeasy FFPE kit (Qiagen, Hilden, Germany) was used according to the manufacturer's protocol. RNA quantification was accomplished using NanoDrop technology (Fisher Scientific, Schwerte, Germany).

miRNA Isolation from Urine

For miRNA isolation from patients' urine, 1 mL of urine was used and added to the Qiazol reagent, mixed, and further used according to the manufacturer's protocol (miRNeasy kit; Qiagen). RNA quantification was accomplished using NanoDrop technology.

Nuclear and Cytoplasmic Isolation

Nuclear and cytoplasmic extracts were isolated from frozen tumor samples, treated cells, or controls, according to the manufacturer's protocol (Nuclear Extraction Kit; Active Motif). Protein content was assayed with the Bradford protein assay (Bio-Rad), with bovine serum albumin as the standard.

PKCα Binding of Pri-miRNA 15a

The NE was isolated (as previously described) from fresh, snap-frozen tumor samples. This extract, 150 μg, was incubated with a PKCα-specific agarose-conjugated antibody (described previously in immunoprecipitation). After the antibody binding procedure, the sample was washed twice with 1× PBS. After the final wash, the total RNA was isolated according to the Qiagen protocol. RNA was quantified, RT-PCR was performed, PCR with primers specific for pri-miRNA 15a detection was performed, and the resulting product of the expected size was Sanger sequenced.

qPCR Data

Of the previously mentioned cDNA, 1 μL was used for quantitative real-time PCR (qPCR) analysis. The experimental settings were as previously described.[20,21]

For quantitative analysis, β-actin was measured. All samples were normalized to β-actin as the reference gene. All experiments were performed in triplicate. Relative fluorescence was calculated using the $\Delta\Delta C_T$ method, as outlined in user bulletin 2 (PE Applied Biosystems, Darmstadt, Germany). The statistical significance of qPCR values at different time points was assessed by the Student's paired *t*-test.

The mirVana qPCR Primer Set for miR-15a was used according to the manufacturer's instructions (Invitrogen). The primer set for 5S ribosomal RNA served to normalize results among different samples. Table 2 provides primer information.

RT-PCR Data

The cDNA was obtained from 250 ng of RNA using random primers and SuperScript III reverse transcriptase, according to the manufacturer's protocol (Invitrogen). The RT-PCR was performed as previously described.[20,21]

Sanger Sequencing

The gel-extracted PCR product from the PKCα agarose antibody immunoprecipitation was prepared for Sanger sequencing according to the BigDye protocol (Applied Biosystems, Darmstadt, Germany). The product was sequenced by the Cologne Center for Genomics and analyzed with the FinchTV version 1.4.0 (Euscan, The Netherlands).

Tissue Array

Formalin-fixed and paraffinized renal (tumor and normal) tissues (listed in Table 1) were pre-evaluated for β-actin by qPCR to ensure good tissue preservation. From those tissues, core punch biopsy samples (each with a 2-mm diameter) were taken and assembled into a paraffin block with prepunched holes to allow simultaneous immunohistological analysis of up to 35 tissue samples at once.

Tumor Regression

Tumor regression as a morphological term is defined by the destruction of the tumor's structure under the appearance of necrosis, massive hemorrhage, and inflammation, as well as subsequent restructuring by scaring.

The tumor samples we defined as regressive showed that >50% of the tumor parenchyma was destroyed in the described manner. More important, this regression occurred as part of normal tumor development. It was not therapeutically induced nor were there detectable reasons for its occurrence, such as vascular thrombosis or external tumor compression. The regression occurred primarily in the center of the tumor, as is known in other tumor entities, so that living tumor cells were only preserved around the edge of the pseudoencapsulated tumors.

Western Blot Analysis

Western blot analysis was performed as previously described.[20,21] For the analysis of the PKC isoforms, antibodies (Santa Cruz) were used and tested for specificity with designed peptides (Santa Cruz).

Statistics

All experiments were performed in triplicate. For the statistical analysis, the GraphPrism 5 program (GraphPad Software, La Jolla, CA) was used. An analysis of variance was performed, and the significant differences were calculated by the Newman-Keuls method and indicated by asterisks. All differences without indication were not statistically significant. The RCC versus RCC regressive differences were analyzed by unpaired *t*-test.

Results

PKC in Renal Tumors

Tissue Array Analysis of PKCα and PKCβ2

To localize PKC isoforms, an immunohistological study using antibodies against PKCα and PKCβII was performed in all paraffin-embedded tissues (n = 28) (Table 1). PKCβ2 was expressed in proximal tubules but not in glomeruli in normal and all four carcinoma subtypes studied. PKCα was identified in proximal tubuli of normal kidneys (n = 5), oncocytoma (n = 5), and papillary RCC (n = 6), but not in clear-cell RCC (n = 7) or CP carcinoma (n = 5) (Figure 1A). PKC isoform

Figure 1. PKC isoforms in renal tumors. **A:** Western blot analysis of PKC isoforms by specific antibodies using protein extracts from frozen renal tumors. β-Actin was used as a loading control. Major differences exist between both tumor types regarding the classical isoforms α and β2. **B:** Representative results for different renal tumors and normal renal tissue of immunohistological features for PKCα and PKCβ2 staining with specific antibodies by tissue array. Five to seven samples of each group were analyzed simultaneously by punch biopsy samples assembled in a tissue array. No PKCα was detectable in RCC and CP. Original magnification: ×40; ×200 (**inset**). CP, chromophobe RCC; Onco, oncocytoma; PAP, papillary RCC.

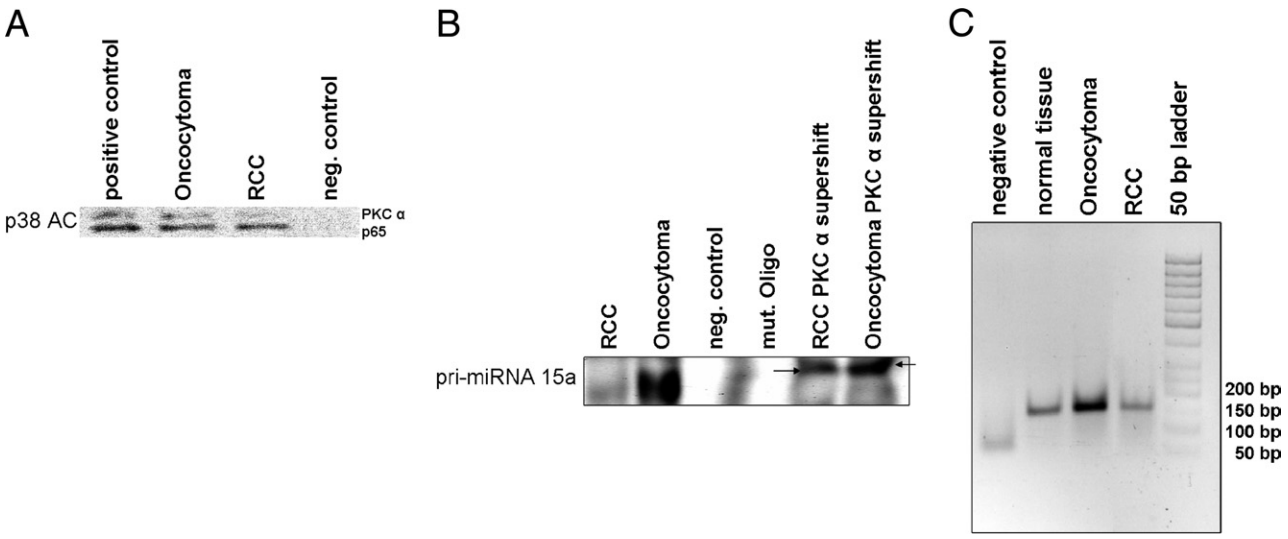

Figure 2. Immunoprecipitation analysis of the TC. **A:** Immunoprecipitation using MAPK p38-coated agarose beads analyzed by using Western blot analysis with specific antibodies (PKCα and p65). Complex formation is detectable in all three samples. **B:** EMSA of NEs from frozen RCC tissue. Pri-miRNA 15a oligonucleotide containing a specific binding site, representing the pre-/pri-miRNA 15a sequence and NEs of used tissues, a potential direct interaction between PKCα and the complex by EMSA is shown. PKCα can be identified as major component by supershift analysis. Specificity determined by 100× unlabeled oligonucleotide. The supershift was performed with a specific anti-PKCα antibody; its specificity was previously analyzed.[34] **C:** Agarose gel electrophoresis showing the expected size of the amplificate at 192 bp in RCCs obtained by PCR after immunoprecipitation using PKCα agarose beads. Control tissue represents nontumorous tissue from the same patient. Only agarose-labeled beads were used as a negative control. mut, mutated (Cy5-5′-GTGTTCGGGGTCCCCTT-3′; MWG, Cologne, Germany); neg, negative.

expression was detectable in equal intensity when present. Results regarded as negative did not reveal any staining throughout the tissue samples analyzed.

PKC Isoforms

Because immunohistological findings indicated a homogeneous expression of PKCα throughout cases of a specific tumor class, frozen tissues from two randomly chosen RCCs and oncocytoma were further studied by using Western blot analysis.

By using specific antibodies for different isoforms, PKC members were identified from cytoplasmic extracts of frozen RCC versus oncocytoma samples. PKCs βI, βII, δ, ε, and μ were detectable, whereas in the benign oncocytoma, PKC isoforms α, βI, little βII, η, and ι could be identified (Figure 1B).

Detection of miRNA 15a and PKCα in Renal Tumors

Immunoprecipitation Analysis of the TC

Immunoprecipitation using MAPK p38-coated agarose beads demonstrates that both NF-κB p65 and PKCα were part of the complex (Figure 2A) in frozen fresh samples from renal tumors. However, the amount of PKCα was reduced in malignant RCC versus being highly prevalent in benign oncocytoma (Figure 1B).

Interaction of PKCα with pri-miRNA 15a

To confirm the interaction between PKCα, we used NEs from renal tumors and an Alexa 667–labeled oligonucleotide representing the sequence of pri-miRNA 15a that is the interaction site between PKCα. Supershift analysis with an antibody specific for PKCα identified this isoform as a component of the observed complex formation (Figure 2B).

To demonstrate the direct interaction between pri-miRNA 15a and PKCα, primers were designed that would specifically amplify a stretch of pri-miRNA 15a with the expected binding site of PKCα.[34] Figure 2C represents the result of agarose gel electrophoresis, showing the expected size of the amplificate at 192 bp. The product was obtained by PCR after an immunoprecipitation, using PKCα agarose beads and NEs from freshly frozen oncocytoma samples, RCC, and control tissue. To control the specificity of the PCR product, the nucleotide sequence

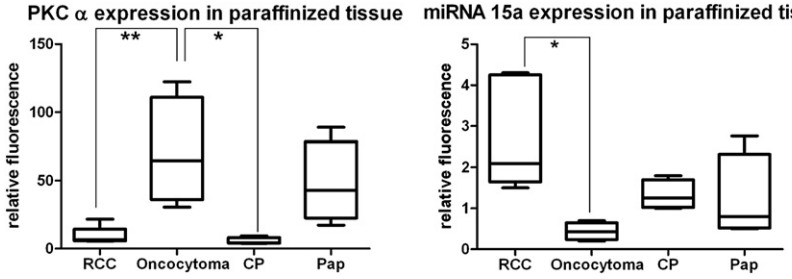

Figure 3. Gene expression levels for different groups of paraffin-embedded renal tumors (Table 1) by box plot analysis. Gene expression of miRNA 15a and PKCα in a set of five to seven samples of each group were analyzed via qPCR. There is an inverse correlation between miRNA 15a and PKCα in RCC versus oncocytoma. CP results closely resemble those of RCC, whereas papillary results are more closely related to those of oncocytoma. CP, chromophobe RCC; Pap, papillary RCC. $^{*}P < 0.05$, $^{**}P < 0.01$.

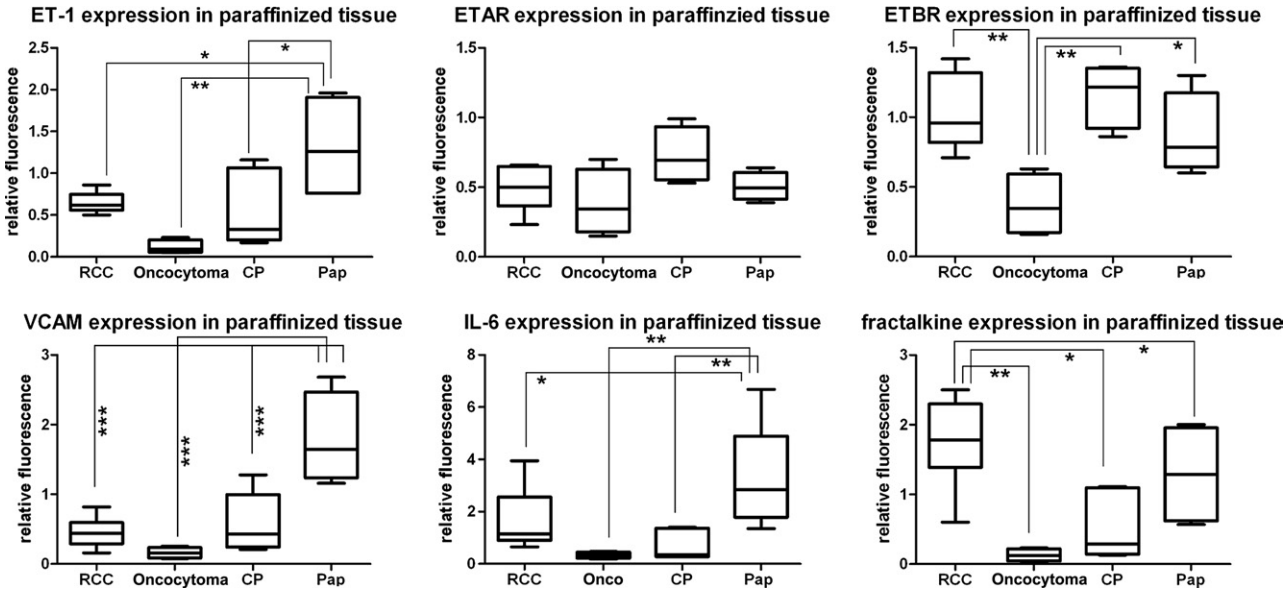

Figure 4. Gene expression levels of ET-1 and the receptors and different NF-κB–dependent target genes for the four different renal tumor subgroups. Results for RCC and CP are closely matched and inversely related to those of oncocytoma. In contrast, in Pap, higher expression levels are detectable than expected from the analysis of signal components in Figure 3A. Box plots display the median (bold line) and the first and third quartile range (box). CP, chromophobe RCC; Onco, oncocytoma; Pap, papillary RCC. $^{*}P < 0.05$, $^{**}P < 0.01$, and $^{***}P < 0.001$.

of the amplificate was analyzed by Sanger sequencing (data not shown).

PKCα and miRNA 15a Expression Levels in Human Renal Tumors

By RT-qPCR, we analyzed the expression levels of PKCα and miRNA 15a (Figure 3) of paraffin-embedded tissues (listed in Table 1). In RCC and CP, the PKCα expression was low; in papillary RCC, it was moderately low; and in oncocytoma, it highly increased. In contrast, miRNA 15a levels were decreased in oncocytoma and papillary RCC and slightly increased in clear-cell RCC and CP.

Target Gene Expression in Human Renal Tumors

By RT-qPCR, we analyzed the expression levels of different NF-κB target genes (Figure 4) of the paraffin-embedded tissues listed in Table 1. Overall, malignant RCCs had the highest expression levels of all tumor groups investigated. Gene levels in CP and papillary RCCs were lower, being lowest in oncocytoma.

miRNA 15a as a Potential Urine Marker to Identify Malignant versus Benign Renal Tumors

Because miRNA could be identified in the urine and malignant RCCs had high levels in their tumor cells (Figure 3), we investigated whether miRNA 15a could serve as a potential marker to differentiate these malignant tumors from benign oncocytomas, by analyzing urine samples from patients with tumors. miRNA 15a was extracted from freshly collected urine from different groups of patients with primary renal tumors, other malignant or benign tumors, or inflammatory conditions, as listed in Table 3. After real-time qPCR analyses of urine from well-preserved clear-cell RCCs, overall high levels of relative fluorescence of miRNA 15a were detectable immediately before operation, which decreased significantly (ie, decreased to nearly to 0 at hospital release; Figure 5A).

Carcinoma of the urogenital tract and other tumors, such as colon cancer and hepatic cell carcinoma, failed to show increased miRNA 15a levels (Figure 5B). Furthermore, inflammatory conditions were equally incapable of increasing miRNA 15a levels (Figure 5B). The increased expression of miRNA 15a in patients' urine with RCCs compared with all other collected urine samples was significant, as indicated by asterisks (Figure 5B). However, urine samples from patients with RCCs with regressive changes affecting >50% of the tumor parenchyma also show significant differences regarding RCCs.

In contrast, clear-cell RCCs with regressive changes affecting >50% of the tumor parenchyma displayed miRNA 15a levels equal to control cases, whereas PKCα levels were increased (Figure 6). $p16^{INK4a}$ was used as a marker for tumor regression (Figure 7), demonstrating that all tumors with increased PKCα levels showed increased expression of $p16^{INK4a}$ as well.

Discussion

As we demonstrated earlier,[20] different normal and tumor cell lines induced a cytoplasmic TC consisting of NF-κB p65–MAPK p38 after ET-1 stimulation, among them Caki-1 cells, an RCC-derived tumor cell line. Furthermore, a signaling loop exists in Caki-1 cells[21,34]; in rest-

Table 3. List of Data for Patients, Their Respective Tumor and Nontumor Diseases, and Results of the Relative Fluorescence Values of miRNA 15a in Urine Used in This Study

Patient no.	Sex	Age (years)	Clinical evidence	Tumor size (cm)	Relative fluorescence
1	F	63	RCC	0.6	166.46
2	M	56	RCC	6.0	18.62
3	F	71	RCC	3.07	248
4	M	75	RCC	3.7	60.08
5	F	81	RCC	3.6	81.8
6	F	70	RCC	3.9	56.06
7	M	60	RCC	3.5	56.8
8	F	64	RCC	5.7	35.2
9	F	55	RCC	11	184.02
10	F	54	RCC	5.5	28.72
11	M	76	Oncocytoma	5.0	0.35
12	M	71	Oncocytoma	1.5	2.38
13	F	70	Oncocytoma	3.2	10.86
14	M	68	Oncocytoma	3.6	1.18
15	M	65	Oncocytoma	3.5	3.35
16	M	47	RCC, regressive	6.0	0.39
17	M	81	RCC, regressive	12.5	4.66
18	M	74	RCC, regressive	6.5	0.96
19	M	69	RCC, regressive	2.2	0.38
20	M	63	RCC, regressive	4.2	5.0
21	M	45	RCC, regressive	6.8	0.46
22	F	69	RCC, regressive	1.9	1.03
23	M	72	RCC, regressive	4.9	1.62
24	F	66	RCC, regressive	6.8	5.97
25	M	86	Urothelial carcinoma		0.97
26	M	67	Urothelial carcinoma		3.15
27	M	70	Urothelial carcinoma		0.36
28	M	78	Urothelial carcinoma		4.37
29	M	63	Urothelial carcinoma		2.95
30	M	70	Prostatitis		1.36
31	F	33	Urinary bladder infection		3.17
32	M	32	Pyelonephritis		6.91
33	M	65	Angiomyolipoma	6.5	1.42
34	M	64	Papillary adenoma, urogenital Tbc		2.97
35	M	59	Hemangioma liver sclerotic, papillary RCC (G_1)		30.1
36	M	68	Liposarcoma		3.17
37	M	78	Colon carcinoma		4.25
38	M	60	Pancreas carcinoma		20.52
39	M	46	Pancreas carcinoma		18.12
40	M	78	HCC		0.86
41	F	58	Colon adenoma		2.57
42	F	63	Lymph cyst		8.13
43	F	58	Cystic nephroma		15.87
44	M	78	Urinary bladder cancer, metastases		4.37
45	F	55	Undifferentiated urogenital tract tumor, metastases		14.84

F, female; M, male; HCC, hepatocellular carcinoma; Tbc, tuberculosis.

ing cells, PKCα associated with the TC is able, after nuclear migration, to suppress the release of pri-miRNA 15a. This miRNA 15a (*MIR15A*) appears necessary to regulate signaling after ET-1 induction: the mediator induces decreasing PKCα levels, which can no longer suppress nuclear pri-miRNA release, resulting in cytoplasmic accumulation of mature miRNA 15a. Because Caki-1 cells are the corresponding malignant cell line to clear-cell RCC, we investigated whether this signaling loop is present in clear-cell and other subtypes of RCC versus benign oncocytoma.

At the start of this investigation, PKCα was not detectable by immune histological characteristics in clear-cell RCC, being in agreement with the findings of Brenner et al.[28] However, a strong signal could be obtained for oncocytoma (Figure 1B). Different PKC isoforms present in renal tumors were identified between clear-cell RCC and oncocytoma from fresh collected tissue samples, using two tumors of each subtype for analysis because of the high degree of homology in immune staining. With this approach, we wanted to analyze whether expression patterns in isoforms could help to explain differences in signaling and subsequent tumor behavior. Interestingly, major differences between our study and those of Engers et al[27] and Brenner et al[28] are the lack of expression of PKCη versus the detectability of the β1 and β2 isoforms in RCCs, but not in oncocytomas by using Western blot analysis and immune histological characteristics (Figure 1). Furthermore, and in contrast to our study, Engert et al[35] did not detect the δ isoform. The reason for these

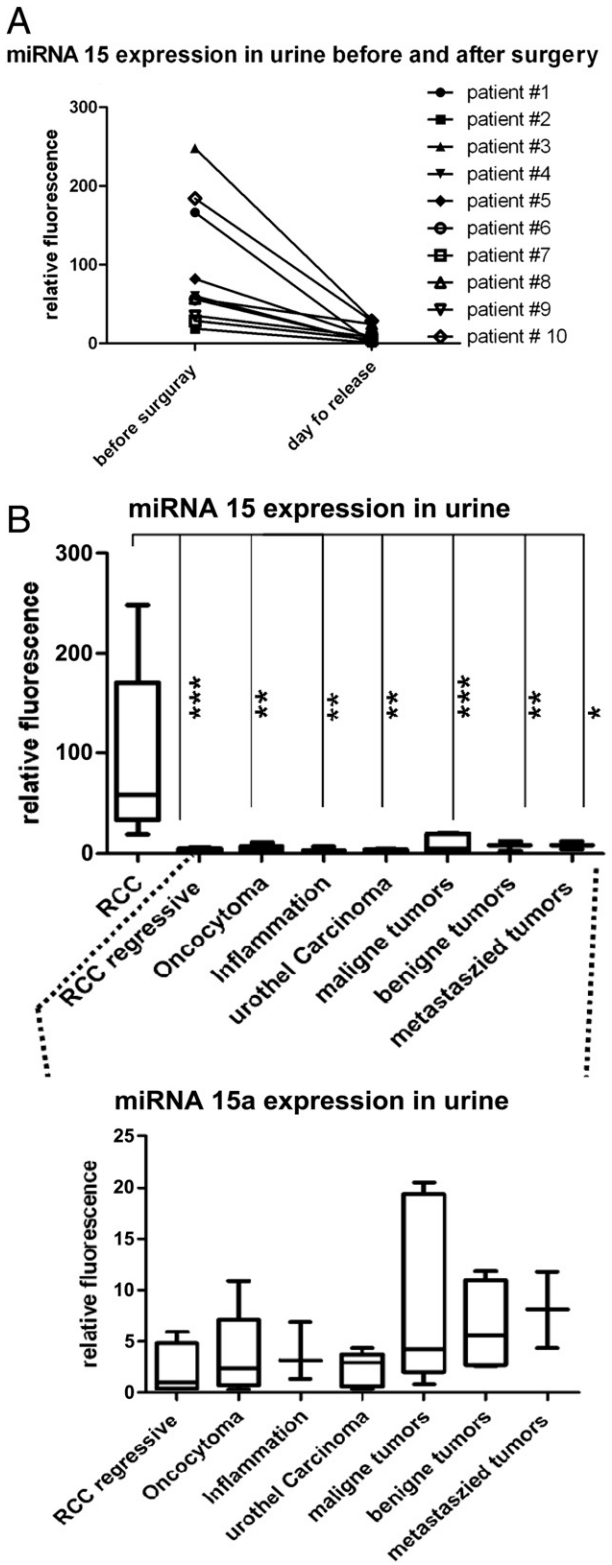

Figure 5. qPCR results using urine from patients listed in Table 3. **A:** Urine from patients with clear-cell renal carcinoma. Preoperatively increased values for urinary miRNA15a levels show a marked decrease postoperatively at hospital release. $P < 0.005$. **B:** Box plot analyses from the urine of patients with different disease entities in the urogenital tract, as listed in Table 1. In contrast to urine from RCCs, urine of the other disease entities analyzed shows median levels of relative fluorescence units of miRNA 15a of ≤10. maligne, malignant tumors; urothel, urothelial. $^{*}P < 0.05$, $^{**}P < 0.01$, and $^{***}P < 0.001$.

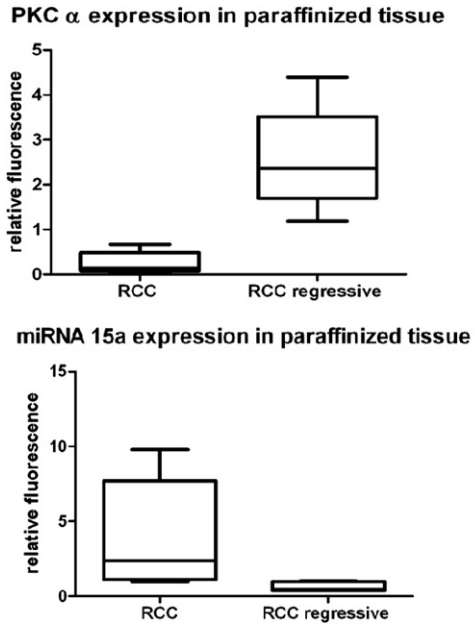

Figure 6. Analysis of levels of PKCα and miRNA 15a in RCCs with minimal (<10%) versus major (≥50%) regressive changes. Marked regressive changes lead to an inverse relationship with levels of high PKCα and low levels of miRNA 15a. $P < 0.05$. The paraffinized tissues used in this experiment are derived from the cases from which urine analysis was performed in Table 3.

discrepancies remains speculative. The use of different antibodies could be one of the most likely reasons, with improved antibodies becoming available since the studies were conducted 7 years ago. Atypical PKC isoforms, however, were not detected by using Western blot analysis in either normal human renal tissue or in human renal tumors. This result differs from reports in the rat kidney, where the major PKC isoform is α, in addition to δ, and ξ, whereas others are not expressed.[36]

One of the major novel and unexpected findings of this article is the inverted relationship between low levels of PKCα and high levels of miRNA 15a in RCCs, compared with previously reported tumor investigations. In the literature, miRNA 15a has been described as a tumor suppressor, promoting apoptosis and inhibiting cell proliferation by targeting multiple oncogenes.[10] The down-regulation of miRNA 15a and 16-1 has consequently been reported in lymphoproliferative

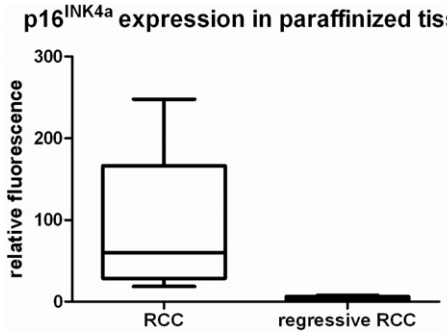

Figure 7. Analysis of levels of p16^{INK4a} in well-preserved versus highly regressive RCCs (>50%) as a marker for regression. $P < 0.001$.

disorders, in multiple myeloma,[11] and in prostate cancer.[12] Furthermore, in oral squamous cell carcinoma, Cohen et al[9] have reported that the up-regulated PKCα isoform is inversely related with a decreased production of miRNA 15a. This discrepancy remains puzzling, particularly because we found similar discrepant relationships between these two factors in cervical carcinoma and melanoma,[34] so that a tumor-specific phenomenon as an explanation seems unlikely.

According to studies with cultured Caki-1 cells, one important question was the identification of the formation of the TC consisting of p65 and p38 components joined by PKC. Although this complex is generally detectable, PKCα can only be detected in oncocytoma in a significant amount (Figure 2A). This indicates that, regarding NF-κB signaling, the situation in oncocytoma resembles closely that in resting Caki-1 cells, whereas RCCs represent the situation after mediator-stimulated signal transduction, in which ET-1 induction has been described as an important mediator.[37] This can be further strengthened by the observation in Figure 2B, in which, by EMSA, with NEs from both tumor types, a complex consisting of PKCα with the oligonucleotide pri-miRNA 15a containing a PKCα homologous nucleotide binding site, can only be identified for oncocytoma, but not for RCC.

In an attempt to validate the importance of the differences in signaling between the malignant RCC subtypes and the benign oncocytoma, we analyzed the expression levels of several known NF-κB target genes that were relevant in previous studies in normal proximal renal tubule cells and their malignant counterparts, the Caki-1 cells.[20,21] For vascular cell adhesion molecule-1, IL-6, and fractalkine, the relationship between higher levels for the clear-cell and CP RCC subtypes, paralleling that for the signaling components compared with the benign oncocytoma, could be confirmed. Unexpectedly, levels of gene expression in the papillary subtype of RCC were relatively high compared with the expected results. Herein, potentially additional pathways may modify the signaling result, which awaits further studies.

Because differences in the behavior of RCCs have been related, in part, to ET-1, we determined levels of gene expression for ET-1 and its two receptors, A and B. Again, the clear-cell and the CP subtype of RCC reveal overall higher levels of ET-1 and its receptors than the oncocytoma samples. The same is true for the lower levels of ET type-B receptor in papillary RCCs. These results are in overall principal agreement with the observation that ET-1 reportedly promotes cell survival in RCCs through the ET-A receptor[31] in different renal tumor cell lines. However, we observed a major discrepancy regarding papillary RCCs. Although major differences in endothelial axis expression seem to exist between clear-cell and papillary subtypes,[32] we found, in contrast to Douglas et al,[32] that a papillary RCC has, on average, more ET-1 and ET-A receptor expression than the clear-cell subtype.

In addition to being an interesting signaling system, the characterization of the individual components, and particularly miRNA 15a, has provided the potential for a new marker differentiating clear-cell RCC from oncocytoma. This differential can be particularly difficult in preoperative, diagnostic renal tumor biopsy samples, because oncocytic features can be found as a minor component in clear-cell RCCs. Herein, the analysis of the miRNA 15a levels could be of significant help, considering that this investigation (if a molecular pathology laboratory is at hand) is, time wise, at least equivalent to the much less informative, albeit nonspecific, immune histological features.

The potentially most relevant role for miRNA 15a as a diagnostic marker, however, is indicated by its detectability in the urine of patients with renal cancer (Figure 5). According to our initial investigation, clear-cell RCCs have distinctly increased miRNA 15a levels compared with those before tumor resection, which decreases, in almost all cases, to background values after operation or at the time of hospital release. In only one case with lymph node metastases, higher levels of miRNA persisted after primary tumor resection. Whether this phenomenon could be used as a diagnostic tool in revealing tumor metastases has to be further evaluated.

The potential applicability of urinary miRNA 15a values for diagnostics is further supported by the fact that other urinary and nonurinary tumors, and inflammatory conditions of the urinary tract, do not seem to cause increased miRNA 15a levels (Figure 5B). Potentially false-negative values may occur. However, in cases with major RCC tumor regression in which miRNA 15a levels remain low, this could be explained by the observation that tumors undergoing apoptotic changes show high PKCα levels, which, according to our model, should result in decreased amounts of detectable miRNA 15a.[38] The $p16^{INK4a}$ tumor suppressor and aging status marker was used to analyze kidney tumor regression.[39] A clear correlation between tumor regression and increased values of $p16^{INK4a}$ was detectable (Figure 7). Whether the correlation between the degree of tumor necrosis and levels of $p16^{INK4a}$ is also linear will depend on reliable data of the amount of necrosis per tumor. For this analysis, further studies are needed, because the data are not available in our databank, because their potential importance has not been recognized.[16]

Thus, although miRNA 15a has, in our opinion, a promising potential as a diagnostic marker, clinical studies with more tumor cases are needed to prove its diagnostic value.

Acknowledgment

This study is dedicated to Dr. Werner Fries, on occasion of his 86th birthday.

References

1. Ambros V: MicroRNA pathways in flies and worms: growth, death, fat, stress, and timing. Cell 2003, 113:673–676
2. Bartel B, Bartel DP: MicroRNAs: at the root of plant development? Plant Physiol 2003, 132:709–717
3. Bartel DP: MicroRNAs: genomics, biogenesis, mechanism, and function. Cell 2004, 116:281–297

4. Palatnik JF, Allen E, Wu X, Schommer C, Schwab R, Carrington JC, Weigel D: Control of leaf morphogenesis by microRNAs. Nature 2003, 425:257–263
5. Lagos-Quintana M, Rauhut R, Meyer J, Borkhardt A, Tuschl T: New microRNAs from mouse and human. RNA 2003, 9:175–179
6. Lim LP, Glasner ME, Yekta S, Burge CB, Bartel DP: Vertebrate microRNA genes. Science 2003, 299:1540
7. Lee Y, Kim M, Han J, Yeom KH, Lee S, Baek SH, Kim VN: MicroRNA genes are transcribed by RNA polymerase II. EMBO J 2004, 23: 4051–4060
8. Calin GA, Sevignani C, Dumitru CD, Hyslop T, Noch E, Yendamuri S, Shimizu M, Rattan S, Bullrich F, Negrini M, Croce CM: Human microRNA genes are frequently located at fragile sites and genomic regions involved in cancers. Proc Natl Acad Sci U S A 2004, 101: 2999–3004
9. Cohen EE, Zhu H, Lingen MW, Martin LE, Kuo WL, Choi EA, Kocherginsky M, Parker JS, Chung CH, Rosner MR: A feed-forward loop involving protein kinase Calpha and microRNAs regulates tumor cell cycle. Cancer Res 2009, 69:65–74
10. Aqeilan RI, Calin GA, Croce CM: miR-15a and miR-16-1 in cancer: discovery, function and future perspectives. Cell Death Differ 2010, 17:215–220
11. Roccaro AM, Sacco A, Chen C, Runnels J, Leleu X, Azab F, Azab AK, Jia X, Ngo HT, Melhem MR, Burwick N, Varticovski L, Novina CD, Rollins BJ, Anderson KC, Ghobrial IM: microRNA expression in the biology, prognosis, and therapy of Waldenstrom macroglobulinemia. Blood 2009, 113:4391–4402
12. Bonci D, Coppola V, Musumeci M, Addario A, Giuffrida R, Memeo L, D'Urso L, Pagliuca A, Biffoni M, Labbaye C, Bartucci M, Muto G, Peschle C, De Maria R: The miR-15a-miR-16-1 cluster controls prostate cancer by targeting multiple oncogenic activities. Nat Med 2008, 14:1271–1277
13. Tong AW, Nemunaitis J: Modulation of miRNA activity in human cancer: a new paradigm for cancer gene therapy? Cancer Gene Ther 2008, 15:341–355
14. Yanagisawa M, Kurihara H, Kimura S, Goto K, Masaki T: A novel peptide vasoconstrictor, endothelin, is produced by vascular endothelium and modulates smooth muscle Ca2+ channels. J Hypertens Suppl 1988, 6:S188–S191
15. Ong AC, Jowett TP, Firth JD, Burton S, Karet FE, Fine LG: An endothelin-1 mediated autocrine growth loop involved in human renal tubular regeneration. Kidney Int 1995, 48:390–401
16. Ong AC, Jowett TP, Firth JD, Burton S, Kitamura M, Fine LG: Human tubular-derived endothelin in the paracrine regulation of renal interstitial fibroblast function. Exp Nephrol 1994, 2:134
17. Bruzzi I, Benigni A: Endothelin is a key modulator of progressive renal injury: experimental data and novel therapeutic strategies. Clin Exp Pharmacol Physiol 1996, 23:349–353
18. Fukuroda T, Fujikawa T, Ozaki S, Ishikawa K, Yano M, Nishikibe M: Clearance of circulating endothelin-1 by ETB receptors in rats. Biochem Biophys Res Commun 1994, 199:1461–1465
19. Kohan DE: Endothelins in the normal and diseased kidney. Am J Kidney Dis 1997, 29:2–26
20. Gerstung M, Roth T, Dienes HP, Licht C, Fries JW: Endothelin-1 induces NF-kappaB via two independent pathways in human renal tubular epithelial cells. Am J Nephrol 2007, 27:294–300
21. von Brandenstein MG, Ngum Abety A, Depping R, Roth T, Koehler M, Dienes HP, Fries JW: A p38-p65 transcription complex induced by endothelin-1 mediates signal transduction in cancer cells. Biochim Biophys Acta 2008, 1783:1613–1622
22. Bradham C, McClay DR: p38 MAPK in development and cancer. Cell Cycle 2006, 5:824–828
23. Vanden Berghe W, Plaisance S, Boone E, De Bosscher K, Schmitz ML, Fiers W, Haegeman G: p38 and extracellular signal-regulated kinase mitogen-activated protein kinase pathways are required for nuclear factor-kappaB p65 transactivation mediated by tumor necrosis factor. J Biol Chem 1998, 273:3285–3290
24. Dekker LV, Parker PJ: Protein kinase C: a question of specificity. Trends Biochem Sci 1994, 19:73–77
25. Hug H, Sarre TF: Protein kinase C isoenzymes: divergence in signal transduction? Biochem J 1993, 291(Pt 2):329–343
26. Nishizuka Y: Protein kinase C and lipid signaling for sustained cellular responses. FASEB J 1995, 9:484–496
27. Engers R, Mrzyk S, Springer E, Fabbro D, Weissgerber G, Gernharz CD, Gabbert HE: Protein kinase C in human renal cell carcinomas: role in invasion and differential isoenzyme expression. Br J Cancer 2000, 82:1063–1069
28. Brenner W, Farber G, Herget T, Wiesner C, Hengstler JG, Thuroff JW: Protein kinase C eta is associated with progression of renal cell carcinoma (RCC). Anticancer Res 2003, 23:4001–4006
29. Brunelli M, Eble JN, Zhang S, Martignoni G, Delahunt B, Cheng L: Eosinophilic and classic chromophobe renal cell carcinomas have similar frequent losses of multiple chromosomes from among chromosomes 1, 2, 6, 10, and 17, and this pattern of genetic abnormality is not present in renal oncocytoma. Mod Pathol 2005, 18:161–169
30. Amin MB, Tamboli P, Javidan J, Stricker H, de-Peralta Venturina M, Deshpande A, Menon M: Prognostic impact of histologic subtyping of adult renal epithelial neoplasms: an experience of 405 cases. Am J Surg Pathol 2002, 26:281–291
31. Pflug BR, Zheng H, Udan MS, D'Antonio JM, Marshall FF, Brooks JD, Nelson JB: Endothelin-1 promotes cell survival in renal cell carcinoma through the ET(A) receptor. Cancer Lett 2007, 246:139–148
32. Douglas ML, Richardson MM, Nicol DL: Endothelin axis expression is markedly different in the two main subtypes of renal cell carcinoma. Cancer 2004, 100:2118–2124
33. Huang D, Ding Y, Luo WM, Bender S, Qian CN, Kort E, Zhang ZF, VandenBeldt K, Duesbery NS, Resau JH, Teh BT: Inhibition of MAPK kinase signaling pathways suppressed renal cell carcinoma growth and angiogenesis in vivo. Cancer Res 2008, 68:81–88
34. von Brandenstein M, Depping R, Schäfer E, Dienes HP, Fries JW: Protein kinase C α regulates nuclear pri-microRNA 15a release as part of endothelin signaling. Biochim Biophys Acta 2011, 1813:1793–1802
35. Engert A, Schiller P, Josting A, Herrmann R, Koch P, Sieber M, Boissevain F, De Wit M, Mezger J, Duhmke E, Willich N, Muller RP, Schmidt BF, Renner H, Muller-Hermelink HK, Pfistner B, Wolf J, Hasenclever D, Loffler M, Diehl V: Involved-field radiotherapy is equally effective and less toxic compared with extended-field radiotherapy after four cycles of chemotherapy in patients with early-stage unfavorable Hodgkin's lymphoma: results of the HD8 trial of the German Hodgkin's Lymphoma Study Group. J Clin Oncol 2003, 21:3601–3608
36. Ostlund E, Mendez CF, Jacobsson G, Fryckstedt J, Meister B, Aperia A: Expression of protein kinase C isoforms in renal tissue. Kidney Int 1995, 47:766–773
37. Nelson J, Bagnato A, Battistini B, Nisen P: The endothelin axis: emerging role in cancer. Nat Rev Cancer 2003, 3:110–116
38. Gonzalez-Guerrico AM, Meshki J, Xiao L, Benavides F, Conti CJ, Kazanietz MG: Molecular mechanisms of protein kinase C-induced apoptosis in prostate cancer cells. J Biochem Mol Biol 2005, 38:639–645
39. Melk A, Schmidt BM, Takeuchi O, Sawitzki B, Rayner DC, Halloran PF: Expression of p16INK4a and other cell cycle regulator and senescence associated genes in aging human kidney. Kidney Int 2004, 65:510–520